Check for updates

Water Practice & Technology

IWA PUBLISHING

© 2024 The Authors

Water Practice & Technology Vol 19 No 2, 401 doi: 10.2166/wpt.2024.029

Removal of pollutants from landfill leachate by adsorption with nano zero-valent iron particles: adsorption isotherms and kinetic studies

Serdar Göçer[a,*], Binnaz Zeynep Zaimoğlu[a] and Kevser Cırık[b]

[a] Department of Environmental Engineering, Çukurova University, Adana, Turkey
[b] Department of Environmental Engineering, Kahramanmaras Sutcu Imam University, Kahramanmaras, Turkey
*Corresponding author. E-mail: serdargocer33@hotmail.com

ABSTRACT

Nano zero-valent iron (nZVI) is an effective adsorbent for removing various organic and inorganic contaminants. In this study, nZVI particles, synthesized in our previous work, were used for landfill leachate pretreatment. The adsorption performance was tested at various adsorbent concentrations (50–500 mg Fe^0/L), pH (3–8), and contact times (15–330 min). Chemical oxygen demand, dissolved organic carbon (DOC), nitrate (NO_3^-), and ammonium (NH_4^+) removal efficiency were approximately 75%, 60, 57, and 33%, respectively. The obtained data were fitted well by the Langmuir isotherm and adsorption kinetics of pseudo-second-order equations ($R^2 > 0.9$). The adsorption capacities were found to be 29.62, 21.01, and 3.12 mg/g for DOC, NH_4^+, and NO_3^-, respectively, at Fe^0 concentration of 50 mg Fe^0/L, pH of 8, and contact time of 120 min, which was determined as the effective operational conditions in this work. The obtained removal levels were higher compared to the conventional activated carbon adsorption (72.3%). Results suggest that nZVI has the potential to create effective adsorption relevant to landfill leachate pretreatment, thereby providing more efficient biological treatment by decreasing important pollutants before biological treatment.

Key words: adsorption, equilibrium isotherms, kinetics, landfill leachate, zero valent iron

HIGHLIGHTS

- Nano zero-valent iron (nZVI) can be used as an effective adsorbent for removing chemical oxygen demand, dissolved organic carbon (DOC), NO_3^-, and NH_4^+ from landfill leachate.
- The adsorption capacities were found to be 29.62, 21.01, and 3.12 mg/g, for DOC, NH_4^+, and NO_3^-, respectively, at an nZVI concentration of 50 mg nZVI/L.
- The obtained data were fitted well by the Langmuir isotherm and adsorption kinetics of pseudo-second-order equations.

1. INTRODUCTION

Adsorption can be defined as the absorption of solutes by liquid or solid surfaces as part of the intermass transport mechanism (Cabooter *et al.* 2021). Adsorption is a significant treatment technology when used singly or in a combined treatment process to remove organic and inorganic substances (Rodriguez *et al.* 2004; Kurniawan & Lo 2009; Kulikowska *et al.* 2016; Lee & Hur 2016; Oloibiri *et al.* 2017). In recent years, nanoparticles (NPs) have been proposed as efficient adsorbents in the remediation of water and soil because of their unique atomic properties, higher reduction capacity, higher removal efficiency, magnetic property, nontoxic, molecular, and chemical properties compared to traditional adsorbents such as granulated-powdered and fiber-activated carbons Granular Activated Carbon (GAC), Powdered Activated Carbon (PAC) and Activated Fiber Carbon (AFC) (Hu *et al.* 2004; Chang & Chen 2005; Yantasee *et al.* 2007; Liu *et al.* 2008; Yuan *et al.* 2010). All these properties can be used in the treatment of different types of wastewaters. There are many reports, where different categories of adsorbents had been used for organic and inorganic pollutants from wastewaters such as activated carbon (AC) (Ai *et al.* 2011), graphenes (Tamer & Berber 2022), ash (Liu *et al.* 2018), agricultural wastes (Crini 2006), biomass (Canizo *et al.* 2019), clay materials (Loqman *et al.* 2017), silica (Li *et al.* 2020a, 2020b), zeolites (Wu *et al.* 2021), acid-based hydrogels (Yuan *et al.* 2019), magnetic-coated biochars (Sun *et al.* 2015), activated alumina (Adak *et al.* 2005), magnetic oxide-based materials (Dutta *et al.* 2021), nonmagnetic iron oxide (Hamidzadeh *et al.* 2015), nanorods (Thattil & Leema Rose 2020), and magnetic calcium ferrite NPs (An *et al.* 2015). In recent years, adsorption processes using iron-based nanomaterials have attracted the attention of researchers due to their high surface area,

This is an Open Access article distributed under the terms of the Creative Commons Attribution Licence (CC BY-NC-ND 4.0), which permits copying and redistribution for non-commercial purposes with no derivatives, provided the original work is properly cited (http://creativecommons.org/licenses/by-nc-nd/4.0/).

Downloaded from http://iwaponline.com/wpt/article-pdf/doi/10.2166/wpt.2024.029/1374706/wpt2024029.pdf
by guest

cost-effectiveness, and properties to remove pollutants from wastewater (Amiri *et al.* 2018 Nisticò & Carlos 2019; Li *et al.* 2020a, 2020b; Yi *et al.* 2020). The commonly used NPs for wastewater treatment are nano zero-valent iron (nZVI), metal oxide NPs, carbon nanotubes, and nanocomposites. Among them, nZVI has achieved very interesting and promising results for various pollutant remediation such as pesticides, polychlorinated hydrocarbons, chlorobenzenes, and coloring agents (Ghasemzadeh *et al.* 2014; Galdames *et al.* 2020). nZVI has been reported to be an environmental friendly material with high reactivity, effective yield, controllable particle size, active site with a diameter ranging from 1 to 100 nm. nZVI also has small size, large specific surface area, and strong reducing capacity (Fan *et al.* 2020; Ken & Sinha 2020). In addition, nZVI has high aggregation due to its high surface area and magnetic properties. High surface area is preferred in the removal of pollutants in wastewater because nZVI has a high adsorption capacity. As a result, a small amount is needed to reduce contaminants in an aqueous solution, thus reducing its cost (Stefaniuk *et al.* 2016; Wang *et al.* 2019).

Landfill leachate (LFL) is very strong wastewater and causes environmental concern due to the wide range of polluting parameters it contains. LFL has a highly contaminated complex content of biodegradable and nonbiodegradable substances (Ziyang *et al.* 2009; de Godoy Leme & Miguel 2018). There are many factors affecting the quality of such leachates, i.e., age, precipitation, seasonal weather variation, waste type, composition, operating procedures, hydrogeological factors, climatic conditions of the region, garbage depth and permeability, storage method, and changes. LFL is dark brown colored and odorous wastewater containing many suspended and dissolved organic substances, pathogenic Fe element content was determined as Biochemical oxygen demand (BOD), chemical oxygen demand (COD), dissolved organic carbon (DOC), nitrogenous compounds (NH_3–N, organic nitrogen, NO_3–N, NH_4^+–N, etc.), heavy metals, and xenobiotics substances (Akkaya & Demir 2009; Atmaca 2009; Gotvajn *et al.* 2009; Lou *et al.* 2009). The age of LFL is classified as young, middle, and mature. Generally, storage age plays an important role in the quality of collected LFL (Renou *et al.* 2008). The age of LFL is determined by the BOD/COD ratio. The BOD/COD ratio for young, medium, and mature has value ranges of 0.5–1.0, 0.1–0.5, and <0.1, respectively. Mature LFL is characterized by organic substances resistant to biodegradation such as humic acid and high concentrations of NH_3–N. As the LFL age increases, the rate of easily decomposed organic substances decreases after completion of biological decomposition (Renou *et al.* 2008). Mature LFL (>10 years) is rich in ammonia nitrogen due to fermentation and hydrolysis of nitrogenous fractions of biodegradable substrates (Nordin 2006). As time progresses, leachate passes through the aerobic, acetogenic, methanogenic, and stabilization stages of organic waste degradation, and in these stages, the properties of leachate such as COD, BOD, BOD/COD ratio, NH_4^+–N, and pH vary considerably (Kjeldsen *et al.* 2002). LFL treatment is very complicated, is expensive, and generally requires a combination of various treatment processes (Bashir *et al.* 2010). Although several methods of LFL treatment are available, adsorption has been widely used as pretreatment or post-treatment due to its simplicity and cost-effectiveness. Furthermore, the adsorption process of LFL by nZVI is preferred comparatively with other treatment methods due to its high efficiency, ease of operation, and ability to wastewater treatment. Also, many isotherm and kinetics models have been proposed for describing mechanisms of NP adsorption from the aqueous solution. However, the report provides practical guidance for choosing an appropriate method by comparing Langmuir and Freundlich isotherm models, and pseudo-first-order and pseudo-second-order models have been tested for modeling the adsorption kinetics of NPs from the aqueous solution (Ruíz-Baltazar *et al.* 2015). Although different isotherm models have been developed to describe the sorption of several pollutants on nZVI, there has been very limited information on adsorption performance toward LFL. Kashitarash *et al.* (2012) reported fast removal efficiency of 47.94% for COD in 10 min at optimal conditions; however, sorption interactions onto nZVI particles have not been included in this study. Thus, for a deeper understanding of the LFL treatment and the related sorption interactions onto nZVI particles, the Langmuir and Freundlich isotherms have been considered in this study. Moreover, pseudo-first-order and pseudo-second-order kinetics models were applied to the sorption data for a deeper insight into the removal mechanism. Conde-González *et al.* (2016) reported that AgNPs, using copper-based metal NP material, fit well with pseudo-second-order and Langmuir models compared to adsorption from aqueous solutions, but that the adsorption did not continue beyond the monolayer, describing the equilibrium behavior better than the Freundlich isotherm. In another study, experimental data for the adsorption of AgNPs on commercial AC showed that the Freundlich isotherm can describe the equilibrium behavior better than the Langmuir isotherm because the adsorption continues beyond the monolayer (Gicheva & Yordanov 2013). Results from different studies have shown that the usefulness of statistical tests in model validation for the adsorption of NPs onto the surface of a material is very limited.

Downloaded from http://iwaponline.com/wpt/article-pdf/doi/10.2166/wpt.2024.029/1374706/wpt2024029.pdf
by guest

The main aim of the present research was to investigate the removal of DOC, COD, NH_4^+, NO_3^-, and color of LFL by applying nZVI as an efficient adsorbent. The suitability of the selected adsorption isotherms (Langmuir and Freundlich) and kinetics (pseduo-first-order and second-order equations) were determined. Moreover, the adsorption mechanism of LFL on the surface of nZVI was investigated in a batch adsorption process. Finally, DOC, COD, NH_4^+, and NO_3^- of LFL and the effect of pH, reaction time, and nZVI concentration variation were investigated to determine the optimum conditions.

2. MATERIALS AND METHODS

2.1. Preparation of nZVI

The nZVI was synthesized with a dispersing agent, polyethylene glycol (PEG-4000). The basic principle of the synthesis was that ferrous ion was rapidly reduced to nZVI by borohydride solution according to the following reaction (Equation (1)) (He *et al.* 2012):

$$Fe^{+}_{2\,(aq)} + 2BH^{-}_{4\,(aq)} + 6H_2O \rightarrow Fe^{0}_{(s)} + 2B(OH)_{3(aq)} + 7H_2 \uparrow \quad (1)$$

In this method, 1.7868 g $FeSO_4{\bullet}7H_2O$ was dissolved in 90 mL 4/1 (v/v) ethanol/deionized water mixture in a 500-mL bottle and then 0.3 g PEG-4000 was added into the aforementioned solution. The temperature was kept at 20 °C. The solution was stirred at 220 rpm for 30 min to ensure that PEG-4000 was completely dissolved. Before reductant addition, the solution pH was adjusted to about 6.5 with 1 M NaOH. Then, 50 mL of 1.3883 g KBH_4 aqueous solution was added dropwise into the mixture at 220 rpm. The solution was stirred for another 30 min after the addition of all KBH_4. Then the resulting black solid particles were washed with deoxygenated water three times and with deoxygenated absolute ethanol two times and were collected by magnetic separation. Finally, the nZVI particles were dried at 70 °C and stored in N_2 gas to prevent nZVI oxidation from atmospheric oxygen. In our previous work, synthesized nZVI characterization was carried out using X-ray diffraction (XRD), scanning electron microscopy with energy dispersive X-ray spectroscopy (SEM-EDX), and Fourier-transform infrared spectroscopy (FTIR) techniques (Göçer *et al.* 2019). According to XRD, the 2θ peak at 44.8096 °, representing 100% intensity, indicates the presence of nZVI NPs in the sample. According to this result, it was observed that nZVI was synthesized successfully and that nZVI showed superiority against oxidation. According to SEM and EDX, the surface roughness of nZVI is indicated to have a core–shell structure, where the shell represents the oxidized part surrounding the Fe core and protects it from further oxidation. Also, based on EDX results of nZVI, the Fe element content was determined to be 98%. The Brunauer-Emmett-Teller (BET) surface area of nZVI was determined to be 36.8063 m^2/g. The peaks indicating the presence of nZVI were detected in FTIR analysis to be between 500 and 1,200 cm^{-1} (Göçer *et al.* 2019).

2.2. Landfill leachate

Raw LFL was collected from a municipal sanitary landfill located in Kahramanmaras, Turkey. The total amounts of LFL deposited daily were 815–830 tons. LFL was collected from the equilibration tank and stored at 4 °C until used. The characteristics of raw LFL are summarized in Table 1. The analyses show the typical characteristics of

Table 1 | Landfill leachate characterization

Parameters (this study)	Concentration (mg/L) (this study)	Concentration (mg/L)	Reference
pH	6.5–7.5	7.7	Lau *et al.* (2001)
DOC	7058 ± 400	1400–11,000 ± 400	Duyar *et al.* (2021)
COD	16,000 ± 1500	10,000–18,000 ± 1500	Çeçen & Aktaş (2004)
BOD	1500 ± 300	2300 ± 300	Lopez *et al.* (2004)
NH_4^+–N	2120 ± 200	2020 ± 200	Ozturk *et al.* (2003)
BOD/COD	0.10 (medium age)	0.19	Li & Zhao (2001)
NO_3^-	670 ± 40	187 ± 40	Duyar *et al.* (2021)
Pt-Co (color unit)	6380 ± 300	Dark brown	Duyar *et al.* (2021)
PO_4^{-3}–P	78 ± 10	32 ± 10	Lopez *et al.* (2004)

Downloaded from http://iwaponline.com/wpt/article-pdf/doi/10.2166/wpt.2024.029/1374706/wpt2024029.pdf
by guest

medium LFLs, with high COD, high ammonium concentration, and BOD/COD ratio 0.10. In general, the pH value in medium LFL is determined as 6.5–7.5 (Table 1). The pH value of experimental sets varied between 3 and 8, by adding 1 M NaOH and 1 M HCl to adsorption experiments.

2.3. Adsorption experiments and capacity

The effect of various parameters such as pH (3–8), contact time (15–330 min), and nZVI concentration (50–500 mgFe^0/L) was tested on NH_4^+, NO_3^-, DOC, and COD removal in batch adsorption experiments, for the evaluation of the optimum process conditions (Table 2). The adsorption tests were performed in 'Jar test' equipment (VELP scientific, JLT 6, Italy), where six simultaneous tests could be performed. The jars tests (500 mL capacity) were submitted to a constant rotation speed of 200 rpm and the total test duration of 330 min. All the experiments were carried out at a laboratory scale using 500 mL Erlenmeyer flasks as batch reactors (Table 2). Batch adsorption tests were conducted to evaluate the isotherms and kinetics of adsorption onto the nZVI adsorbents at 25 °C (room temperature). Stock solutions of nZVI were prepared by dissolving 1.7868 g $FeSO_4.7H_2O$ in 90 mL 4/1 (v/v) ethanol/deionized water mixture in a 500-mL bottle. A calibration curve was then created based on 10 concentrations (range, 0–500 mg/L) at 25 °C. Five concentrations (50–50 mg/L) of the solutions described earlier were prepared in 500-mL bottle. Using 50–100 mg/L nZVI, 500 mL of each LFL wastewater was added, followed by the jar test experiment stirring at pH 3–8 and 200 rpm for 330 min at room temperature (25 °C). After the adsorption experiment, 20 mL of the solutions were centrifuged for 10 min at 3,500 rpm using a centrifuge.

Table 2 | Experimental plan

Nano zero-valent iron (nZVI)	Adsorbent concentration (mgFe^0/L)	pH	Mixing rate (rpm)	Contact time (min)	Temperature (°C)	Volume (mL)
	50	3 4 5 6 7 8	200	15–330	Room temperature (25 °C)	500
	100	3 4 5 6 7 8				
	200	3 4 5 6 7 8				
	300	3 4 5 6 7 8				
	400	3 4 5 6 7 8				
	500	3 4 5 6 7 8				

The adsorption capacity, q_e, (mg g^{-1}), and pollutant removal efficiency (%) of the tested nZVI were calculated by Equations (2) and (3), respectively:

$$\text{Adsorption capacity } (q_e) = \frac{(C_o - C_e) \times V}{W} \tag{2}$$

$$\text{Removal efficiency } (\%) = \frac{(C_o - C_e)}{C_o} \times 100\% \tag{3}$$

In Equations (2) and (3), V is the volume of the leachate (L), W is the amount of adsorbent (g), and C_o and C_e are the initial and equilibrium concentrations of pollutants (mg L^{-1}) in the leachate, respectively.

2.4. Analyses

All samples were centrifuged at 4,000 rpm for 5 min (Eppendorf Centrifuge 5415R, Hamburg, Germany) and then were filtered using a sterile syringe 0.45 μm filter (Sartorius AG, Gottingen, Germany). Dissolved oxygen carbon (DOC) and Total nitrogen (TN) DOC and TN concentrations were analyzed using a TOC instrument coupled with TN (Shimadzu TOC-VCPN, Kyoto, Japan). The pH was measured by a pH meter (Thermo, Orion 4 Star, Indonesia). The ionic composition of influent and effluent samples (ammonium, nitrate) was measured by ion chromatography (Dionex ICS-3000, Sunnyvale, CA, USA). The COD measurements were carried out according to the dichromate-closed reflux colorimetric method described in Standard Methods (Standard Methods, 5220 D). The color was analyzed as Pt-Co units. Pt-Co color measurements were performed spectrophotometrically at 465 nm during lab-scale studies.

Downloaded from http://iwaponline.com/wpt/article-pdf/doi/10.2166/wpt.2024.029/1374706/wpt2024029.pdf
by guest

3. ADSORPTION ISOTHERMS AND KINETICS

The Langmuir and Freundlich isotherms and pseudo-first-order and pseudo-second-order kinetics models were selected to simulate the isotherm adsorption of nZVI in this work.

3.1. Adsorption kinetics

The amount of nZVI absorbed on the pollutants was calculated using Equation (4):

$$q_e = (C_o - C_t) * \frac{V}{m} \tag{4}$$

where q_e expresses the adsorption capacity (mg g^{-1}) and C_0 and C_t are pollutant concentrations (such as DOC, COD, NH_4^+, and NO_3^-) (mg L^{-1}) at time 0 and t, respectively. V indicates the volume of solution (mL) and m is the mass of nZVI (g). Adsorption kinetic parameters are divided into two: pseudo-first-order equations (Ho 2004) and pseudo-second-order equations (Azizian 2004; Ho 2006).

3.1.1. Pseudo-first-order kinetics

The so-called first-order equation (Lagergren's equation) is expressed as the adsorption of solid–liquid solutions based on the adsorption capacity of solids (Ho 2004). The linear form of the so-called first-order model can be expressed by the following equation (Equation (5)):

$$\mathrm{Log}(q_e - q_t) = \mathrm{Log}\, q_e - \left(\frac{k_1}{2.303}\right)t \tag{5}$$

where q_e and q_t (mg g^{-1}) are defined as the adsorption capacities at time $t(h)$ at equilibrium, respectively.

3.1.2. Pseudo-second-order kinetics

The pseudo-second-order kinetics are used to define chemical adsorption from liquid solutions (Azizian 2004; Ho 2006). The linear expression of this kinetics is shown in Equation (6):

$$\frac{t}{q_t} = \frac{1}{[k_2 q_e^2]} + \frac{1}{(q_e)t} \tag{6}$$

where k_2 is the rate constant for pseudo-second-order adsorption (g mg^{-1} h^{-1}) and $k_2 q_e^2$ is the initial adsorption rate (mg g^{-1} h^{-1}).

3.2. Adsorption isotherm models

3.2.1. Freundlich isotherm

Freundlich isotherm models are valid for both monolayer (chemisorption) and multilayer adsorption processes. This isotherm is known adsorbing to the heterogeneous surface of an adsorbent. The linear form of the Freundlich equation is expressed as (Equation (7)) follows:

$$\mathrm{Ln}\, q_e = \mathrm{Ln}K_F + \frac{1}{n}\mathrm{Ln}C_e \tag{7}$$

where K_F and n are Freundlich isotherm constants related to adsorption capacity and adsorption intensity, respectively, and C_e is the equilibrium concentration (mg L^{-1}) (Tan & Xiao 2009).

3.2.2. Langmuir isotherm

The Langmuir isotherm assumes monolayer adsorption on a single surface with a certain number of adsorption sites. After the adsorption zone is filled, no more tendency takes place. In this way, it will reach a saturation point where maximum adsorption of the surface will be achieved. The linear form of the Langmuir isotherm model is expressed as follows (Equation (8)):

$$\frac{C_e}{q_e} = \frac{C_e}{q_{\max}} + \frac{1}{KLq_{\max}} \tag{8}$$

Downloaded from http://iwaponline.com/wpt/article-pdf/doi/10.2166/wpt.2024.029/1374706/wpt2024029.pdf
by guest

where K_L is the Langmuir constant related to the energy of adsorption and q_m is the maximum adsorption capacity (mg g^{-1}) (Chingombe *et al.* 2006; Barkat *et al.* 2009).

4. RESULTS AND DISCUSSION

4.1. Adsorption experiments and capacities

In the adsorption experiments, optimum conditions were examined for different pH values (3–8) and contact time (15–330 min). In terms of COD, optimum conditions were determined at pH and contact time of 8 and 120 min, respectively. The highest COD removal efficiency was about 60%. After that, the effect of increasing zero-valued iron concentration (50–500 mg/L, Table 2) on pollutant removal was tested at a pH of 8 and contact time of 120 min. Optimum zero-valent iron concentration was 50 mg/L in terms of COD, DOC, NH_4^+, and NO_3^-, corresponding to removal of 75, 60, 57, and 33%, respectively. Figure 1 shows the effect of increasing nZVI concentration on the adsorption capacity (q_e). The increase in nZVI from 50 to 500 mg/L decreased the adsorption capacity of pollutants, which may be attributed to the collection of the NPs. According to Figure 1, nZVI adsorption capacity for DOC, NH_4^+, and NO_3^- were found to be 29.62, 21.01, and 3.12 mg/g at 50 mg/L nZVI concentration, respectively. Adly *et al.* (2022) reported that they investigated the removal of phosphorus adsorption on nZVI/AC composite. They found that the maximum adsorption capacity at pH 4 was 53.76 mg/g. They obtained high adsorption capacity due to the use of nZVI and AC as a support material. In another study, biochar prepared with nZVI and sewage sludge was used for arsenic removal from aqueous solutions. They found a relatively higher adsorption capacity (60.61 mg/g) compared to our results, which was probably due to the adverse effect of the strong and the complicated LFL (Liu *et al.* 2021).

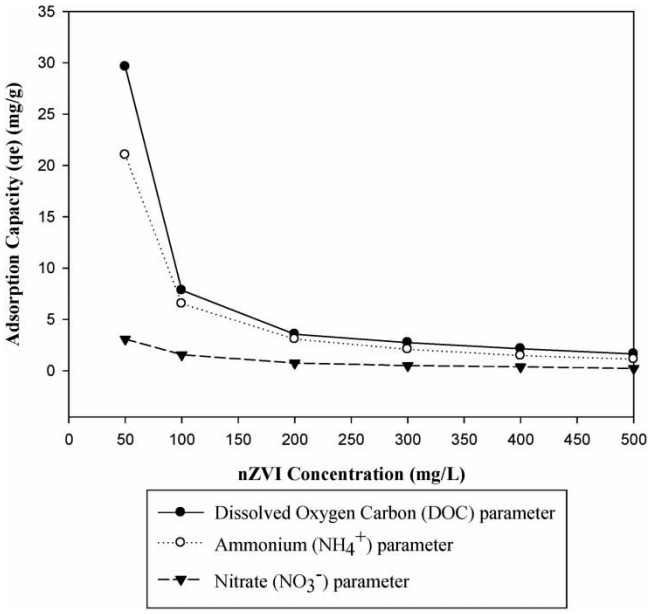


Figure 1 | Effect of nZVI concentration on the adsorption capacity (q_e) for DOC, NH_4^+, and NO_3^- by nZVI particles.

Adsorption of pollutants may decrease at lower and higher pH values (Zou *et al.* 2016). At lower pH values, the adsorption of metal ions is low due to increased nZVI corrosion. According to our study, it was observed that adsorption was effective at high pH. However, at lower pH, the nZVI surface will be positively charged, and this will negatively affect the adsorption of iron ions (Zou *et al.* 2016). It is clear that the removal efficiency increases with increasing nZVI concentrations. Removal efficiencies and adsorption capacities ranging from 50 to 500 mg/L nZVI concentrations are quite low (Figure 1). According to adsorption experiments, it is observed that the efficiency and adsorption capacity remain constant after 15 min of contact time. The results were similar to the previous studies (Efecan *et al.* 2009; Poguberovic *et al.* 2016; Rathor *et al.* 2017; Ulucan-Altuntas *et al.* 2017). While the removal efficiency of increasing nZVI concentration up to 500 mg/L within the same contact

Downloaded from http://iwaponline.com/wpt/article-pdf/doi/10.2166/wpt.2024.029/1374706/wpt2024029.pdf
by guest

time increases almost linearly, it continues at a low angle after 50 mg/L nZVI concentration. On the other hand, it was observed that as the amount of adsorbent increased, the adsorption capacity decreased. A literature review of studies using AC reported that it is necessary to select high adsorbent concentrations in order to have high removal efficiency (Kadirvelu *et al.* 2001; Yavuz *et al.* 2003; Onundi *et al.* 2010; Wang *et al.* 2010a, 2010b). However, in our study, effective results were observed at a concentration of 50 mg/L nZVI.

Halim *et al.* (2010) reported that adsorption capacities of composite medium, zeolite, and AC were 32.89, 17.45, and 6.08 mg/g, respectively, which is in good agreement with our study. Eljamal *et al.* (2022) reported that NPs have great potential for the practical applications of pollutant removal from wastewater. Unlike our study, according to the study by Boparai *et al.* (2011), nZVI particles reported removal of Cd^{2+} in the concentration range of 25–450 mg/L. The maximum adsorption capacity of nZVI for Cd^{2+} was determined as 769.2 mg/g. They reported that nZVI can be used as an efficient adsorbent for the removal of cadmium from polluted water sources. Ashrafi *et al.* (2017) reported in a similar study using Fe_3O_4@MnO_2 core-shell magnetic NPs that optimum times for adsorption were reached in 60 min. Altuntas *et al.* (2018) reported in their study that while they achieved a removal efficiency of 24% by using AC as an adsorbent for nickel removal, they achieved a removal efficiency of approximately 80% with 200 mg/L nZVI. On the other hand, in the study where AC–nZVI NPs containing certain amounts of AC were used, it was observed that the removal efficiency increased up to 99% (Altuntas *et al.* 2018). A range of biodegradable, nonbiodegradable, and humic substances are detected in LFL (Lai *et al.* 2007; Jun *et al.* 2009) and contribute to the COD pollutants. Wang *et al.* (2010a, 2010b) obtained approximately 56 and 50% COD removal efficiency, respectively, by using mango peel nano zero valent iron (MP-nZVI) and starch nano zero valent iron (S-nZVI) modifications as adsorbents in their study. According to the results obtained, it is thought that the removal efficiency of COD increases with the adsorption of the organic compound and its precipitation with iron corrosion products. Also, nitrogen-based compounds are also pollutants found in LFL and cause serious environmental consequences. The removal efficiency of magnetic adsorbents varies depending on the adsorbent structure and pollutants used. In addition, temperature, pH, ionic strength, reaction time, adsorbent concentration, the presence of pollutants, and some other factors also play important roles. In this study, the effects of nZVI adsorbent material on LFL are given with examples. However, very few studies have been conducted using magnetic adsorbents to treat real LFL (Zhang *et al.* 2016, 2018). One study observed that approximately 30% of COD was removed from real LFL by adsorption onto magnetite (Augusto *et al.* 2019). In another study, a combination of oxidation and adsorption of mature LFL using magnetic $CuFe_2O_4$/Reduce Graphene Oxide (RGO) nanocatalyst was also reported (Karimipourfard *et al.* 2019). Unlike our study, Wang *et al.* (2023) obtained an adsorption capacity of 210.9 mg/g by using PS-HQ-HCP (phenolic hydroxyl-functionalized hyper-cross-linked polymers) as an adsorbent in their study.

4.2. Adsorption isotherms

Adsorption isotherms are a widely used method to determine the isotherm equilibrium condition of an adsorption system. Also this method helps to decide the surface area of the adsorbent; the volume, size, and distribution of the pores; the temperature of adsorption; and the absorbability of a gas or vapor on the adsorbent. Adsorption of DOC, NO_3^-, and NH_4^+ by nZVI particles was modeled using the Freundlich and Langmuir isotherms with the quality of the fit assessed using the correlation coefficient (Figures 2–4). Isotherm parameters in terms of DOC are given in Table 3.

The slope and intercept of plots of C_e/q_e versus C_e, at adsorbent concentration, were used to calculate q_m and K_L (Figure 2(a)). The size of $q_{\max}$ and K_L indicates high adsorption capacity (50 mg/L adsorption concentration, Table 3). Adsorption is low if $K_LC_e \ll 1$ and high if $K_LC_e \gg 1$. Table 3 shows that K_LC_e is $\gg 1$ and the amount of adsorption is high. The adsorption process is inconvenient if R_L is greater than 1, it is linear if R_L is equal to 1, it is convenient if R_L is between 0 and 1, and it is irreversible if R_L is 0 (Equation (7)). When the Langmuir isotherm is examined, it is observed that the R_L value is between 0 and 1 (Table 3). The Freundlich isotherm constants K_F and n are determined from the intercept and slope of a plot of $\mathrm{Ln}q_e$ versus $\mathrm{Ln}C_e$ (Figure 2(b)). It is $1/n$ from the slope of the $\mathrm{Ln}C_e$ graph against $\mathrm{Ln}q_e$ and $\mathrm{Ln}K_F$ from the cutting point of the y-axis (Equation (6)). The high $\mathrm{Ln}K_F$ and n values show that sorbent has a high tendency to adsorption and adsorption capacity. The value of $1/n$ ranging from 0 to 1 is expressed as a measure of an adsorption tendency, and heterogeneity becomes heterogeneous as it approaches zero. $1/n < 1$ indicates compatibility with Langmuir isotherm, and $1/n > 1$ indicates compatibility with adsorption condition. As a result, it is observed that the DOC removal adapts to the Langmuir isotherm. The best adsorption capacity suitable for the Langmuir isotherm occurred at a concentration of 50 mg/L nZVI

Downloaded from http://iwaponline.com/wpt/article-pdf/doi/10.2166/wpt.2024.029/1374706/wpt2024029.pdf
by guest

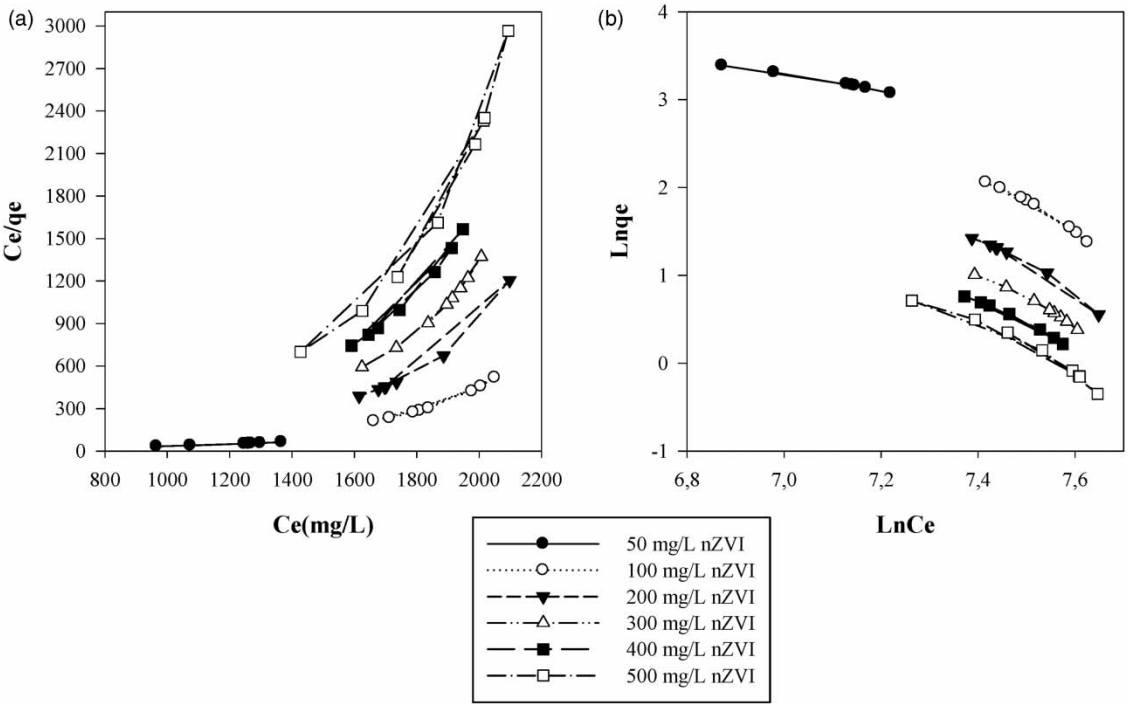


Figure 2 | (a) Langmuir isotherms with DOC removal and (b) Freundlich isotherms with DOC removal.

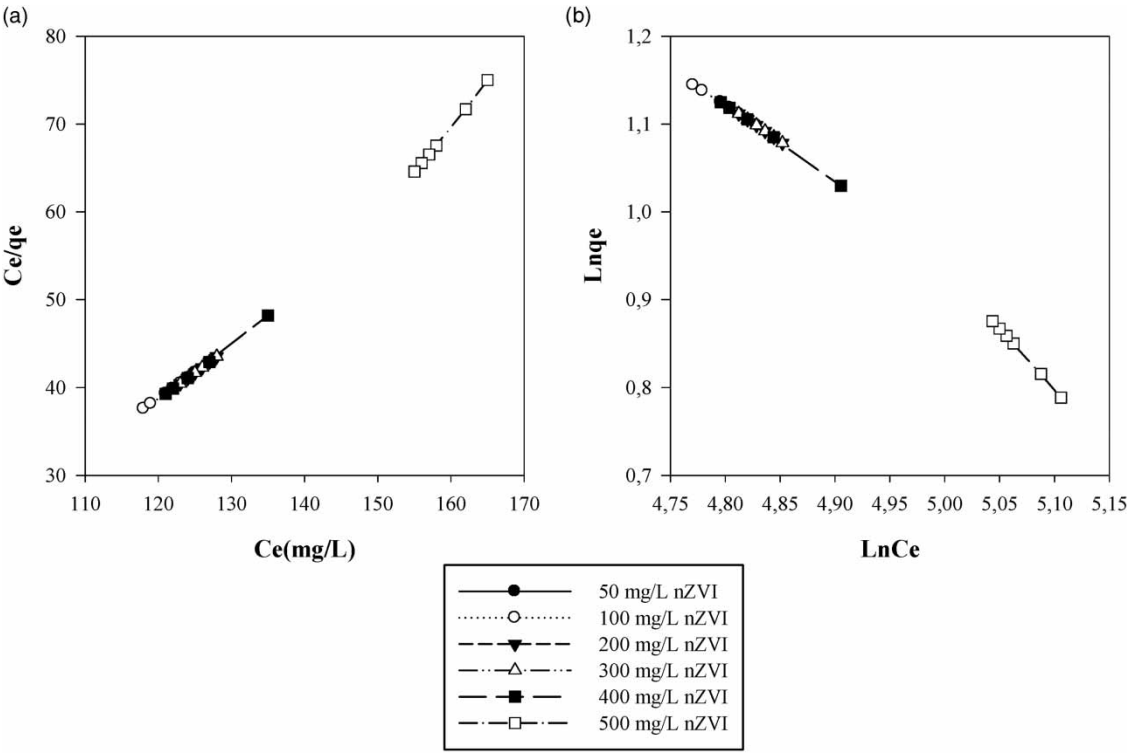


Figure 3 | (a) Langmuir isotherms with NO_3^- removal and (b) Freundlich isotherms with NO_3^- removal.

($R^2 > 0.9931$). Langmuir isotherm parameter fits (Table 3) for DOC removal efficiency adsorption on nZVI yielded isotherms that were in good agreement with observed behavior ($R^2 \geq 0.99$). Maamoun *et al.* (2021) investigated the suitability of various adsorption isotherms and kinetic models to explain the removal of phosphorus (P) from aqueous solutions by nZVI. They found that the Langmuir isotherm and the pseudo-second-order kinetic

Downloaded from http://iwaponline.com/wpt/article-pdf/doi/10.2166/wpt.2024.029/1374706/wpt2024029.pdf
by guest

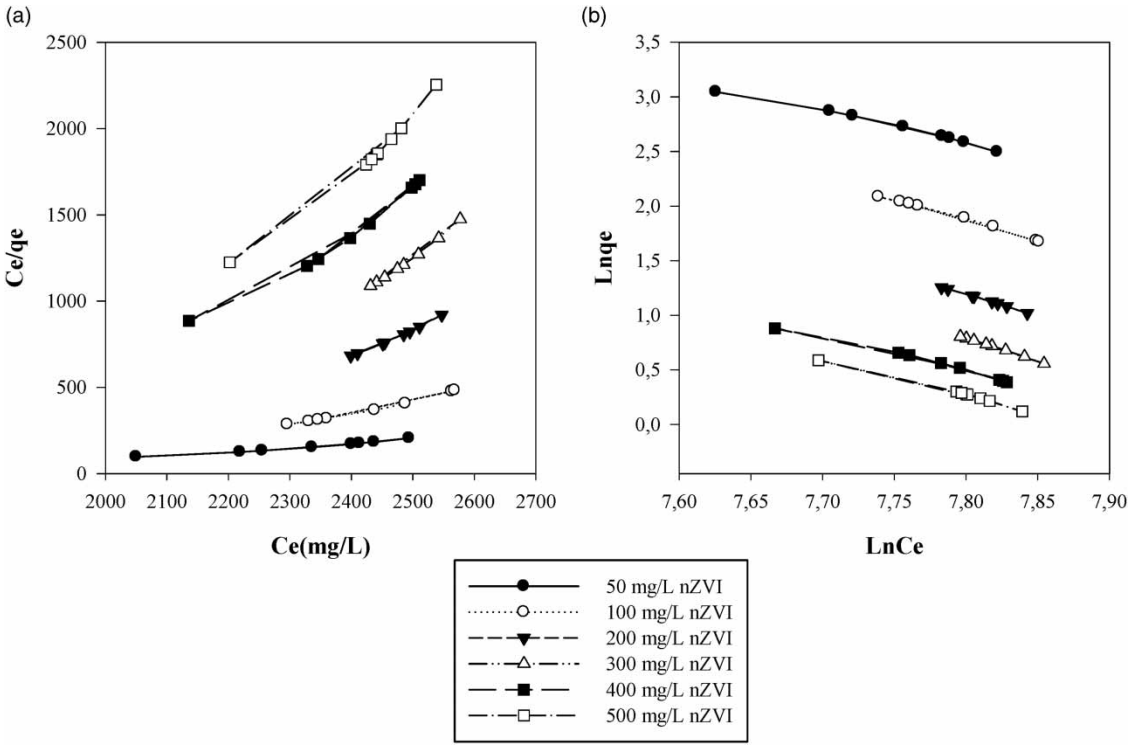


Figure 4 | (a) Langmuir isotherms with NH_4^+ removal and (b) Freundlich isotherms with NH_4^+ removal.

Table 3 | Adsorption isotherms parameters (DOC parameter)

Adsorbent concentration (mg/L)	Langmuir isotherms							Freundlich isotherms			
	Slope	K_L	q_{max}	R_L	R^2	$K_L.C_e$	q_e	Slope	K_F	n	R^2
50	0.0756	3.25	13.22	0.00056	0.9931	1765.95	13.22	−0.9014	1.574	−1.109	0.9927
100	0.7835	3.64	1.276	0.00013	0.971	7211.41	1.276	−3.2661	1.261	−0.306	0.9866
200	1.6968	0.276	0.588	0.00011	0.9573	7211.41	0.588	−3.3491	1.173	−0.298	0.9799
300	0.4893	5.12	2.04	0.0022	0.9669	448.224	2.04	−2.9702	2.341	−0.342	0.9858
400	2.2328	4.339	0.447	0.00017	0.9839	5787.6	0.447	2.6268	1.07	−0.38	0.9922
500	3.2552	1.83	0.307	0.00015	0.923	6555.25	0.307	−2.735	1.015	−0.365	0.9632

model are the best models with the highest linear and nonlinear correlation (R^2). Similarly, in another study, the adsorption capacities of synthesized modified adsorbent (nZVI/AC) for arsenite and arsenate at pH 6.5 calculated from Langmuir adsorption isotherms in batch experiments were 18.2 and 12.0 mg/g, respectively. It can be concluded that nZVI without the use of support material reached the similar results due to its positive effect (Zhu *et al.* 2009). Adsorption of NO_3^- by nZVI particles was modeled using the Freundlich and Langmuir isotherms with the quality of the fit assessed using the correlation coefficient (Figure 3(a) and 3(b)). Isotherm parameters in terms of NO_3^- removal efficiency are listed in Table 4. Altuntas *et al.* (2018) reported in their study that the adsorption capacity was increased from 125 and 820 mg/g for AC and nZVI, respectively, to 1,190 mg/g for 50% AC–nZVI. They also reported that they found the Freundlich model to be the model that best represents isotherm modeling for nZVI. In another study, the adsorption isotherm and kinetic equations using aminated chitosan and graphene oxide-modified adsorbent are similar to our study (Yi *et al.* 2020).

It was observed that NO_3^- removal is fitted to the Freundlich isotherm (Figure 3(b)). In addition, $K_L C_e$ is $\gg 1$, and the amount of adsorption is high. According to the Langmuir isotherm, it was observed that the R_L value is between 0 and 1 (Table 4) confirming that the Langmuir isotherm is suitable for NO_3^- removal. The high $\mathrm{Ln}K_F$ and n values show that sorbent has a high tendency for high adsorption capacity. Unlike our study, Kanel *et al.*

Downloaded from http://iwaponline.com/wpt/article-pdf/doi/10.2166/wpt.2024.029/1374706/wpt2024029.pdf
by guest

Table 4 | Adsorption isotherms parameters (NO_3^- parameter)

	Langmuir isotherms							Freundlich isotherms			
Adsorbent concentration (mg/L)	Slope	K_L	q_{max}	R_L	R^2	$K_L.C_e$	q_e	Slope	K_F	n	R^2
50	0.5935	1.82	1.67	0.0045	0.9999	220.2	1.67	−0.8096	1.26	−1.23	0.9999
100	0.5769	1.78	1.73	0.0046	0.9999	211.82	1.73	−0.781	1.264	−1.28	0.9999
200	0.6166	1.84	1.62	0.0043	0.9999	231	1.62	−0.8412	1.253	−1.18	0.9999
300	0.6166	1.84	1.62	0.0043	0.9999	234	1.62	−0.8412	1.253	−1.18	0.9999
400	0.6367	1.92	1.57	0.0042	0.9994	234.24	1.57	−0.8688	1.256	−1.151	0.9993
500	1.0433	2.43	0.958	0.0024	0.9995	400.95	0.958	−1.3999	1.181	−0.71	0.9996

(2005) investigated arsenic removal efficiency in groundwater by using nZVI as an adsorbent and observed 3.5 mg As(III)/g adsorption capacity with Freundlich isotherm. Other studies using new composite materials for LFL treatment found different results. Langmuir and Freundlich reported that the isotherm's regression coefficients (R^2) for COD and ammonia nitrogen were 0.9971 and 0.9914, respectively (Detho *et al.* 2021). Hashemi *et al.* (2021) investigated ammonium removal efficiency from LFL (LL) using montmorillonite/hematite nanocomposite (M/HNC). They reported that the ammonium adsorption data on the NP material agreed with the Langmuir isotherm models. Isotherm parameters in terms of NH_4^+ removal efficiency are presented in Table 5.

Table 5 | Adsorption isotherms parameters (NH_4^+ parameter)

	Langmuir isotherms							Freundlich isotherms			
Adsorbent concentration (mg/L)	Slope	K_L	q_{max}	R_L	R^2	$K_L.C_e$	q_e	Slope	K_F	n	R^2
50	0.2399	3.56	4.16	0.00013	0.9725	7298	4.16	−2.7844	1.421	−0.359	0.9872
100	0.7312	4.8	1.36	0.00008	0.9899	11942.4	1.36	−3.7169	1.276	−0.269	0.9959
200	1.5718	4.95	0.636	0.00008	0.9944	12300.7	0.636	−3.9212	1.158	−0.255	0.9978
300	2.6273	5.31	0.38	0.00007	0.9949	13142.2	0.38	−4.1943	1.094	−0.238	0.9981
400	2.2266	3.8	0.449	0.0001	0.9737	9541.8	0.449	−3.0823	1.074	−0.324	0.9881
500	2.9092	3.83	0.343	0.0001	0.9747	9720.5	0.343	−3.1881	1.037	−0.313	0.9905

In terms of NH_4^+ removal efficiency and zero-valued iron concentration, it was observed that it fits the Freundlich isotherm (Figure 4(b)). The size of q_{max} and K_L in Langmuir isotherm indicates high adsorption capacity (Table 5). When all these results were examined, Langmuir and Freundlich isotherm equations are created upon ammonium removal and with increasing adsorbent concentrations. These results showed that the optimum condition for adsorption capacity and isotherms was 50 mg/L nZVI ($R^2 > 0.9$). Mittal (2006) used chicken feathers as an adsorbent for the removal of toxic substances containing dye waters. Additionally, it was reported that Langmuir-Freundlich fits adsorption isotherm models. According to our study, similar results were obtained in terms of both removal efficiency and adsorption isotherms. In another study, the adsorption capacities of As(III) and As(V) were 35.83 and 29.04 mg g^{-1}, respectively, as determined from Langmuir adsorption isotherms in batch experiments (Wang *et al.* 2014). When compared with our study, it is seen that the adsorption capacity is high. Similarly, in another study, lead and cadmium adsorption efficiency from leachate by the natural zeolite clinoptilolite was investigated, and they found that best isotherm model for lead adsorption fits the Freundlich model and that for cadmium fits the Langmuir model (Faraji *et al.* 2012).

4.3. Adsorption kinetics

The adsorption rate is a vital parameter to assess the efficiency of an adsorbent for the removal of contaminates. The adsorption of nitrate (NO_3^-), ammonium (NH_4^+), and DOC onto the nZVI was explained through pseudo-first-order and pseudo-second-order kinetic models. The pseudo-first-order kinetic model examines the change in adsorption capacity depending on time. Kinetics parameters in terms of DOC, nitrate (NO_3^-), and ammonium

Downloaded from http://iwaponline.com/wpt/article-pdf/doi/10.2166/wpt.2024.029/1374706/wpt2024029.pdf
by guest

(NH_4^+) removal efficiency are given in Figures 5–7(a) and 7(b). k_1 and q_e, at the adsorbent concentration evaluated experimentally, were calculated using the slope and intercept of plots of $\log(q_e - q_t)$ versus t (Figure 5(a) and Table 6) (Equations (4) and (5)). Pseudo-second-order adsorption parameters q_e and k_2 in Equation (5) were determined by plotting t/q_t versus t (Table 6).

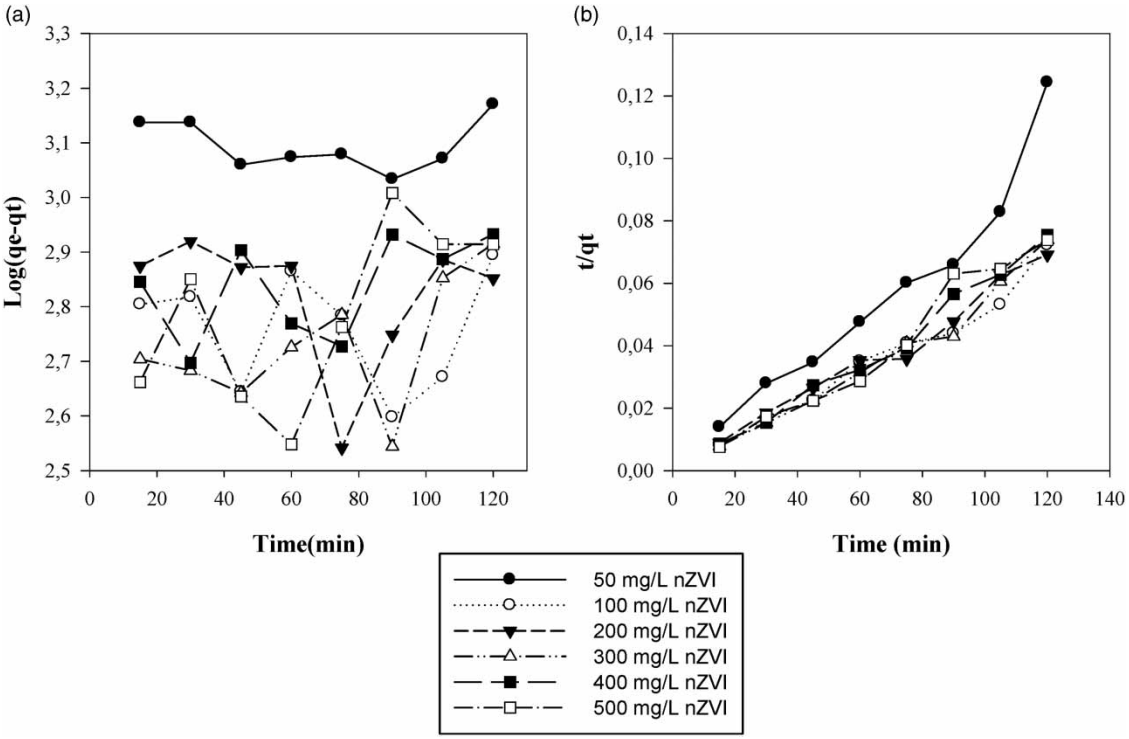


Figure 5 | (a) Pseudo-first-order kinetics with DOC removal and (b) pseudo-second-order kinetics with DOC removal.

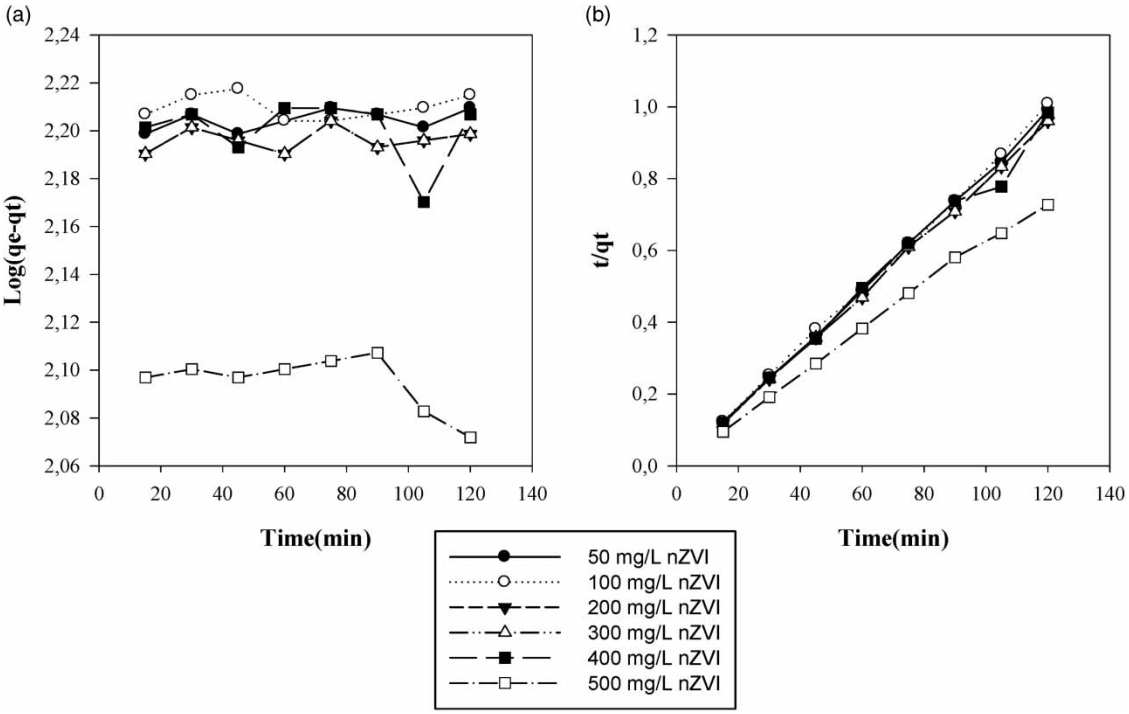


Figure 6 | (a) Pseudo-first-order kinetics with NO_3^- removal and (b) pseudo-second-order kinetics with NO_3^- removal.

Downloaded from http://iwaponline.com/wpt/article-pdf/doi/10.2166/wpt.2024.029/1374706/wpt2024029.pdf
by guest

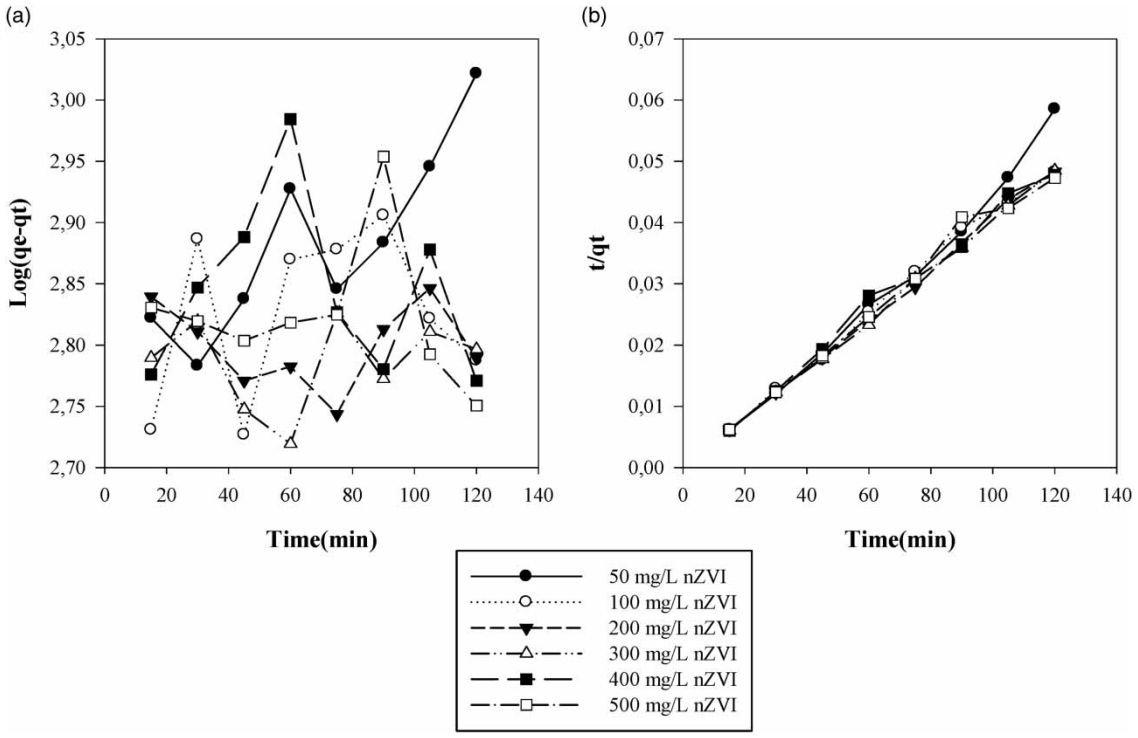


Figure 7 | (a) Pseudo-first-order kinetics with NH_4^+ removal and (b) pseudo-second-order kinetics with NH_4^+ removal.

Table 6 | Adsorption kinetics parameters (DOC parameter)

	Pseudo-first-order kinetics			Pseudo-second-order kinetics		
Adsorbent concentration (mg/L)	Slope (k_1)	q_e (mg/mg)	R^2	Slope (q_e)	k_2	R^2
50	−0.0001	0.0364	0.0114	0.0009	0.0009	0.9233
100	−0.0003	0.0324	0.0073	0.0006	0.0005	0.9673
200	−0.0008	0.033	0.00594	0.0006	0.0005	0.9673
300	0.0017	0.0336	0.2662	0.0006	0.0006	0.973
400	0.0013	0.0336	0.2487	0.0006	0.0006	0.9853
500	0.0027	0.0333	0.3835	0.0007	0.0006	0.9656

Considering the adsorbent concentration and DOC removal efficiency, the R^2 value is very close to 1 in the pseudo-second-order adsorption kinetic equation ($R^2 = 0.9853$, 400 mg/L Fe^0) (Table 6). However, DOC was complied with pseudo-second-order adsorption kinetics (Figure 5(b) and Table 6). These results show that pseudo-second-order kinetics are adsorbed onto the nZVI surface via chemical interaction. Foul *et al.* (2009) investigated the removal efficiency of LFL using two different adsorbents (AC and limestone). Adsorption kinetics, on the other hand, determined their suitability to the pseudo-second-order kinetic model. Similarly, Boparai *et al.* (2011) used nZVI particles to investigate the removal of Cd^{2+} (25–450 mg L^{-1}). They observed that the adsorption kinetics was well adapted using a pseudo-second-order kinetic model. In another study, they aimed to achieve both anionic and cationic dye removal efficiency by using a zero-valent iron-loaded composite NP material. The adsorption process of both dyes was well fitted with the Langmuir isotherm model and pseudo-second-order kinetic model (Eltaweil *et al.* 2021).

The rate parameters of these adsorption kinetic models listed in Tables 7 and 8 indicate that the adsorption of ammonia and nitrate from aqueous solution on nZVI obeys the pseudo-second-order kinetic model according to R^2 (>0.99) (Figures 6 and 7). Previous studies have reported that the adsorption of ammonia on zeolite obeys the pseudo-second-order model (Doğan *et al.* 2005; Lei *et al.* 2008). Genethliou *et al.* (2021) used natural zeolite for the removal of pollutants in raw LFL. They reported that it was mostly suitable for the linear pseudo-second order

Downloaded from http://iwaponline.com/wpt/article-pdf/doi/10.2166/wpt.2024.029/1374706/wpt2024029.pdf
by guest

Table 7 | Adsorption kinetics parameters (NO_3^- parameter)

	Pseudo-first-order kinetics			Pseudo-second-order kinetics		
Adsorbent concentration (mg/L)	**Slope (k_1)**	**q_e (mg/mg)**	**R^2**	**Slope (q_e)**	**k_2**	**R^2**
50	–	0.0259	0.2654	0.0082	0.0082	0.9995
100	–	0.026	0.0002	0.0083	0.0083	0.9991
200	–	0.0258	0.0449	0.008	0.008	0.9994
300	–	0.0258	0.0449	0.008	0.008	0.9994
400	–	0.0259	0.0511	0.0079	0.008	0.991
500	−0.0002	0.0246	0.3195	0.0061	0.0062	0.9974

Table 8 | Adsorption kinetics parameters (NH_4^+ parameter)

	Pseudo-first-order kinetics			Pseudo-second-order kinetics		
Adsorbent concentration (mg/L)	**Slope (k_1)**	**q_e (mg/mg)**	**R^2**	**Slope (q_e)**	**k_2**	**R^2**
50	0.0018	0.0018	0.07231	0.0005	0.0005	0.989
100	0.0005	0.0333	0.0647	0.0004	0.0004	0.9946
200	–	0.0329	0.0051	0.0004	0.0004	0.9983
300	0.0001	0.0328	0.0218	0.0004	0.0004	0.9989
400	−0.0003	0.0334	0.021	0.0004	0.0004	0.9895
500	−0.0002	0.0332	0.0143	0.0004	0.0004	0.9875

model with NH_4^+-N adsorption. In another study, activated biochar-loaded nano zero-valent iron (A-BC-NZVI) was used to remove uranium from wastewater. They found that it complies with the pseudo-second-order equation, and the maximum U(VI) adsorption amount of the Langmuir model at pH 6.0 was 331.13 mg/g (Zhang *et al.* 2021).

Yoon *et al.* (2014) reported in their study that the pseudo-second-order model and Freundlich isotherms were the most appropriate model. Sun *et al.* (2020) reported in their study that the DOC, NH_4^+, and Total Phosphorus (TP) removal efficiencies using electrodes from LFL were 72, 98, and 98%, respectively. They also reported fit to pseudo-first-order and pseudo-second-order kinetic models for DOC, NH_4^+, and TP pollutants. It is similar to our study. Mortazavian *et al.* (2018) reported in their study that it was suitable for pseudo-second-order kinetics and Freundlich isotherm for both AC and AC/nZVI adsorbents. In another study, they reported that the adsorption of Cr(VI) on AC/Fe_2O_3 composite conformed to the Langmuir isotherm model ($R^2 = 0.98$) and pseudo-second-order kinetic model ($R^2 = 0.99$) (Sahu *et al.* 2023). In another study, adsorption of nZVI reported that it was in accordance with second-order kinetic equations and Langmuir isotherm (Delnavaz & Kazemimofrad 2020). Khadim *et al.* (2022) in their study, the adsorption experiment continued for 1 h, while in our study, it was allowed to continue for 5.5 h. Mahdi *et al.* (2023) reported that their study was similar to our study in terms of kinetics and isotherm, but they used different adsorbents as mesoporous material MCM-48. As a result, the adsorption process has been widely used in the removal of organic and inorganic substances. For this reason, it has been reported that it occurs by adsorption to the surface of a highly porous structure through physical and chemical bonds (Foo & Hameed 2009). NPs, which are easy to operate, widely available, and have low synthesis costs, have recently been used in adsorption processes. One of the main advantages of iron and iron-based metal oxide compounds is that they do not lose their magnetic properties during the thermal regeneration process (Peng *et al.* 2006). It has been reported that treatment of LFL using the adsorption process gives successful results, especially in the removal of organic compounds and ammonia nitrogen (Foo & Hameed 2010).

5. CONCLUSION

nZVI can be used as an effective adsorbent for removing COD, DOC, NO_3^-, and NH_4^+ from LFL. Equilibrium isotherms in this study were analyzed using Langmuir and Freundlich models. Kinetic data were obtained and

Downloaded from http://iwaponline.com/wpt/article-pdf/doi/10.2166/wpt.2024.029/1374706/wpt2024029.pdf
by guest

analyzed using pseudo-first-order and pseudo-second-order equations. Optimum conditions were determined as pH 8, reaction time 120 min, and adsorbent dose 50 mg/L nZVI. COD, DOC, NO_3^-, and NH_4^+ removal efficiency was approximately 75, 60, 57, and 33%, respectively. DOC, NH_4^+, and NO_3^- adsorption capacities, respectively, were 29.62, 21.01, and 3.12 mg/g. The experimental results were applied to isotherms commonly used in LFL, and the most suitable isotherm was found to be Langmuir. As a result of administering the experimental data to the kinetic equation, the mechanism controlling the rate was determined, and the most suitable model was found to be the pseudo-second-order equation. Sorption kinetics is investigated to develop an understanding of controlling reaction pathways and the mechanisms of sorption reactions. In the near future, NPs may turn out to be the essential and indispensable components of water and wastewater treatment systems and facilities. The use of nanoparticulate substances, especially nZVI, can partially reduce the concentration of pollutants to meet the final discharge. Therefore, natural nZVI adsorbent may be a suitable alternative in the significant treatment of LFL and pre-treatment or post-treatment. This study demonstrated that nZVI could be applied as adsorbents for pollutant treatment from aqueous solutions.

ACKNOWLEDGEMENTS

This article was supported by the Scientific Research Unit of the Çukurova University. Project No: FDK-2019-11782.

DATA AVAILABILITY STATEMENT

All relevant data are included in the paper or its Supplementary Information.

CONFLICT OF INTEREST

The authors declare there is no conflict.

REFERENCES

Adak, A., Bandyopadhyay, M. & Pal, A. 2005 Removal of crystal violet dye from wastewater by surfactant-modified alumina. *Separation and Purification Technology* **44**(2), 139–144.

Adly, A., Mostafa, N.G. & Elawwad, A. 2022 Adsorption of phosphorus onto nanoscale zero-valent iron/activated carbon: removal mechanisms, thermodynamics, and interferences. *Water Reuse* **12**(1), 111–130.

Ai, L., Li, M. & Li, L. 2011 Adsorption of methylene blue from aqueous solution with activated carbon/cobalt ferrite/alginate composite beads: Kinetics, isotherms, and thermodynamics. *Journal of Chemical & Engineering Data* **56**(8), 3475–3483.

Akkaya, E. & Demir, A. 2009 Energy content estimation of municipal solid waste by multiple regression analysis. In *5th International Advanced Technologies Symposium (IATS'09)*, pp. 13–15.

Altuntaş, K., Debik, E. & Gungor, S. 2018 Nano zero-valent iron supported on activated carbon: effect of AC/nZVI ratio on removal of nickel ion from water. *Global Nest Journal*, **20**(2), 424–431.

Amiri, M. J., Roohi, R. & Gil, A. 2018 Numerical simulation of Cd (II) removal by ostrich bone ash supported nanoscale zero-valent iron in a fixed-bed column system: Utilization of unsteady advection-dispersion-adsorption equation. *Journal of Water Process Engineering* **25**, 1–14.

An, S., Liu, X., Yang, L. & Zhang, L. 2015 Enhancement removal of crystal violet dye using magnetic calcium ferrite nanoparticle: Study in single-and binary-solute systems. *Chemical Engineering Research and Design* **94**, 726–735.

Ashrafi, A., Rahbar-Kelishami, A. & Shayesteh, H. 2017 Highly efficient simultaneous ultrasonic assisted adsorption of Pb (II) by Fe_3O_4@MnO_2 core-shell magnetic nanoparticles: Synthesis and characterization, kinetic, equilibrium, and thermodynamic studies. *Journal of Molecular Structure* **1147**, 40–47.

Atmaca, E. 2009 Treatment of landfill leachate by using electro-Fenton method. *Journal of Hazardous Materials* **163**(1), 109–114.

Augusto, P. A., Castelo-Grande, T., Merchan, L., Estevez, A. M., Quintero, X. & Barbosa, D. 2019 Landfill leachate treatment by sorption in magnetic particles: Preliminary study. *Science of the Total Environment* **648**, 636–668.

Azizian, S. 2004 Kinetic models of sorption: A theoretical analysis. *Journal of Colloid and Interface Science* **276**, 47–52.

Barkat, M., Nibou, D., Chearouche, S. & Mellah, A. 2009 Kinetics and thermodynamics studies of chromium(VI) ions adsorption onto activated carbon from aqueous solutions. *Chemical Engineering and Processing* **48**, 38–47.

Bashir, M. J., Aziz, H. A., Yusoff, M. S. & Adlan, M. N. 2010 Application of response surface methodology (RSM) for optimization of ammoniacal nitrogen removal from semi-aerobic landfill leachate using ion exchange resin. *Desalination* **254**(1–3), 154–161.

Boparai, H. K., Joseph, M. & O'Carroll, D. M. 2011 Kinetics and thermodynamics of cadmium ion removal by adsorption onto nano zerovalent iron particles. *Journal of Hazardous Materials* **186**(1), 458–465.

Cabooter, D., Song, H., Makey, D., Sadriaj, D., Dittmann, M., Stoll, D. & Desmet, G. 2021 Measurement and modelling of the intra-particle diffusion and b-term in reversed-phase liquid chromatography. *Journal of Chromatography A* **1637**, 461852.

Downloaded from http://iwaponline.com/wpt/article-pdf/doi/10.2166/wpt.2024.029/1374706/wpt2024029.pdf
by guest

Canizo, B. V., Agostini, E., Wevar Oller, A. L., Dotto, G. L., Vega, I. A. & Escudero, L. B. 2019 Removal of crystal violet from natural water and effluents through biosorption on bacterial biomass isolated from rhizospheric soil. *Water, Air, & Soil Pollution* **230**, 1–14.

Çeçen, F. & Aktaş, Ö. 2004 Aerobic co-treatment of landfill leachate with domestic wastewater. *Environmental Engineering Science* **21**(3), 303–312.

Chang, Y. C. & Chen, D. H. 2005 Preparation and adsorption properties of monodisperse chitosan-bound Fe_3O_4 magnetic nanoparticles for removal of Cu (II) ions. *Journal of colloid and interface science* **283**(2), 446–451.

Chingombe, P., Saha, B. & Wakeman, R. J. 2006 Sorption of atrazine on conventional and surface modified activated carbons. *Journal of Colloid and Interface Science* **302**, 408–416.

Conde-González, J. E., Peña-Méndez, E. M., Rybáková, S., Pasán, J., Ruiz-Pérez, C. & Havel, J. 2016 Adsorption of silver nanoparticles from aqueous solution on copper-based metal organic frameworks (HKUST-1). *Chemosphere* **150**, 659–666.

Crini, G. 2006 Non-conventional low-cost adsorbents for dye removal: A review. *Bioresource Technology* **97**(9), 1061–1085.

De Godoy Leme, M. A. & Miguel, M. G. 2018 Permeability and retention to water and leachate of a compacted soil used as liner. *Water, Air and Soil Pollution* **229**(11), 1–19.

Delnavaz, M. & Kazemimofrad, Z. 2020 Nano zerovalent iron (NZVI) adsorption performance on acidic dye 36 removal: Optimization of effective factors, isotherm and kinetic study. *Environmental Progress & Sustainable Energy* **39**(4), e13349.

Detho, A., Daud, Z., Rosli, M. A., Ridzuan, M. B., Awang, H., Kamaruddin, M. A. & Halim, A. A. 2021 COD and ammoniacal nitrogen reduction from stabilized landfill leachate using carbon mineral composite adsorbent. *Desalination and Water Treatment* **210**, 143–151.

Doğan, K., Yunus, K., Mustafa, T. & Bulent, A. 2005 Removal of ammonium ion from aqueous solution using natural Turkish clinoptilolite. *Journal of Hazardous Materials* **136**, 604–609.

Dutta, S., Gupta, B., Srivastava, S. K. & Gupta, A. K. 2021 Recent advances on the removal of dyes from wastewater using various adsorbents: A critical review. *Materials Advances* **2**(14), 4497–4531.

Duyar, A., Ciftcioglu, V., Cirik, K., Civelekoglu, G. & Uruş, S. 2021 Treatment of landfill leachate using single-stage anoxic moving bed biofilm reactor and aerobic membrane reactor. *Science of the Total Environment* **776**, 145919.

Efecan, N., Shahwan, T., Eroglu, A. E. & Lieberwirth, I. 2009 Characterization of the uptake of aqueous Ni^{2+} ions on nanoparticles of zero-valent iron (nZVI). *Desalination* **249**(3), 1048–1054.

Eljamal, O., Eljamal, R., Maamoun, I., Khalil, A. M., Shubair, T., Falyouna, O. & Sugihara, Y. 2022 Efficient treatment of ammonia-nitrogen contaminated waters by nano zero-valent iron/zeolite composite. *Chemosphere* **287**, 131990.

Eltaweil, A. S., El-Tawil, A. M., Abd El-Monaem, E. M. & El-Subruiti, G. M. 2021 Zero valent iron nanoparticle-loaded nanobentonite intercalated carboxymethyl chitosan for efficient removal of both anionic and cationic dyes. *ACS Omega* **6**(9), 6348–6360.

Fan, C., Chen, N., Qin, J., Yang, Y., Feng, C., Li, M. & Gao, Y. 2020 Biochar stabilized nano zero-valent iron and its removal performance and mechanism of pentavalent vanadium (V (V)). *Colloids and Surfaces A: Physicochemical and Engineering Aspects* **599**, 124882.

Faraji, M., Mehrizi, E. A., Sadani, M., Karimaei, M., Ghahramani, E., Ghadiri, K. & Taghizadeh, M. S. 2012 Isotherms and kinetics of lead and cadmium uptake from the waste leachate by natural and modified clinoptilolite. *International Journal of Environmental Health Engineering* **1**(1), 26.

Foo, K. Y. & Hameed, B. H. 2009 An overview of landfill leachate treatment via activated carbon adsorption process. *Journal of Hazardous Materials* **171**, 54–60.

Foo, K. Y. & Hameed, B. H. 2010 Insights into the modeling of adsorption isotherm systems. *Chemical Engineering Journal* **156**(1), 2–10.

Foul, A. A., Aziz, H. A., Isa, M. H. & Hung, Y. T. 2009 Primary treatment of anaerobic landfill leachate using activated carbon and limestone: Batch and column studies. *International Journal of Environment and Waste Management* **4**(3–4), 282–298.

Galdames, A., Ruiz-Rubio, L., Orueta, M., Sánchez-Arzalluz, M. & Vilas-Vilela, J. L. 2020 Zero-valent iron nanoparticles for soil and groundwater remediation. *International Journal of Environmental Research and Public Health* **17**(16), 5817.

Genethliou, C., Triantaphyllidou, I. E., Giannakis, D., Papayianni, M., Sygellou, L., Tekerlekopoulou, A. G. & Vayenas, D. V. 2021 Simultaneous removal of ammonium nitrogen, dissolved chemical oxygen demand and color from sanitary landfill leachate using natural zeolite. *Journal of Hazardous Materials* **406**, 124679.

Ghasemzadeh, G., Momenpour, M., Omidi, F., Hosseini, M. R., Ahani, M. & Barzegari, A. 2014 Applications of nanomaterials in water treatment and environmental remediation. *Frontiers of Environmental Science & Engineering* **8**(4), 471–482.

Gicheva, G. & Yordanov, G. 2013 Removal of citrate-coated silver nanoparticles from aqueous dispersions by using activated carbon. *Colloids and Surfaces A: Physicochemical and Engineering Aspects* **431**, 51–59.

Göçer, S., Kozak, M., Akgül, V., Duyar, A., Zaimoğlu, Z. & Cırık, K. 2019 Synthesıs of Nanoscale Zero-Valent Iron (nZVI). In: *International Symposium on Advanced Engineering Technologies (ISADET)*, 2-4 May 2019, Kahramanmaraş/Turkey, pp. 828–833.

Gotvajn, A. Z., Tisler, T. & Zagorc-Koncan, J. 2009 Comparison of different treatment strategies for industrial landfill leachate. *Journal of Hazardous Materials* **162**(2–3), 1446–1456.

Halim, A. A., Aziz, H. A., Johari, M. A. M. & Ariffin, K. S. 2010 Comparison study of ammonia and COD adsorption on zeolite, activated carbon and composite materials in landfill leachate treatment. *Desalination* **262**(1–3), 31–35.

Downloaded from http://iwaponline.com/wpt/article-pdf/doi/10.2166/wpt.2024.029/1374706/wpt2024029.pdf
by guest

Hamidzadeh, S., Torabbeigi, M. & Shahtaheri, S. J. 2015 Removal of crystal violet from water by magnetically modified activated carbon and nanomagnetic iron oxide. *Journal of Environmental Health Science and Engineering* **13**, 1–7.

Hashemi, H., Bahrami, S., Emadi, Z., Shariatipor, H. & Nozari, M. 2021 Optimization of ammonium adsorption from landfill leachate using montmorillonite/hematite nanocomposite: Response surface method based on central composite design. *Desalination and Water Treatment* **232**, 39–54.

He, P., Wang, X., Liu, Y., Liu, X. & Yi, L. 2012 Comparison of electrocatalytic activity of carbon-supported Au–M (M = Fe, Co, Ni, Cu and Zn) bimetallic nanoparticles for direct borohydride fuel cells. *International Journal of Hydrogen Energy* **37**(16), 11984–11993.

Ho, Y. S. 2004 Citation review of Lagergren kinetic rate equation on adsorption reactions. *Scientometrics* **59**, 171–177.

Ho, Y. S. 2006 Review of second-order models for adsorption systems. *Journal of hazardous materials* **136**(3), 681–689.

Hu, J., Johnston, K. P. & Williams III, R. O. 2004 Nanoparticle engineering processes for enhancing the dissolution rates of poorly water soluble drugs. *Drug development and industrial pharmacy* **30**(3), 233–245.

Jun, D., Yongsheng, Z., Weihong, Z. & Mei, H. 2009 Laboratory study on sequenced permeable reactive barrier remediation for landfill leachate-contaminated groundwater. *Journal of Hazardous Materials* **161**, 224–230. doi:10.1016/j.jhazmat.2008.03.086.

Kadirvelu, K., Thamaraiselvi, K. & Namasivayam, C. 2001 Adsorption of nickel(II) from aqueous solution onto activated carbon prepared from coirpith. *Separation and Purification Technology* **24**(3), 497–505.

Kanel, S. R., Manning, B., Charlet, L. & Choi, H. 2005 Removal of arsenic (III) from groundwater by nanoscale zero-valent iron. *Environmental Science & Technology* **39**(5), 1291–1298.

Karimipourfard, D., Eslamloueyan, R. & Mehranbod, N. 2019 Novel heterogeneous degradation of mature landfill leachate using persulfate and magnetic $CuFe_2O_4$/RGO nanocatalyst. *Process Safety and Environmental Protection* **131**, 212–222.

Kashitarash, Z. E., Taghi, S. M., Kazem, N., Abbass, A. & Alireza, R. 2012 Application of iron nanaoparticles in landfill leachate treatment-case study: Hamadan landfill leachate. *Iranian Journal of Environmental Health Science & Engineering* **9**(1), 1–5.

Ken, D. S. & Sinha, A. 2020 Recent developments in surface modification of nano zero-valent iron (nZVI): Remediation, toxicity and environmental impacts. *Environmental Nanotechnology, Monitoring & Management* **14**, 100344.

Khadim, A. T., Albayati, T. M. & Saady, N. M. C. 2022 Removal of sulfur compounds from real diesel fuel employing the encapsulated mesoporous material adsorbent Co/MCM-41 in a fixed-bed column. *Microporous and Mesoporous Materials* **341**, 112020.

Kjeldsen, P., Barlaz, M. A., Rooker, A. P., Baun, A., Ledin, A. & Christensen, T. H. 2002 Present and long-term composition of MSW landfill leachate: A review. *Critical Reviews in Environmental Science and Technology* **32**(4), 297–336.

Kulikowska, D., Bernat, K., Parszuto, K. & Sulek, P. 2016 Efficiency and kinetics of organics removal from landfill leachate by adsorption onto powdered and granular activated carbon. *Desalination and Water Treatment* **57**(10), 4458–4468.

Kurniawan, T. A. & Lo, W. H. 2009 Removal of refractory compounds from stabilized landfill leachate using an integrated H_2O_2 oxidation and granular activated carbon (GAC) adsorption treatment. *Water research* **43**(16), 4079–4091.

Lai, P., Zhao, H. Z., Wang, C. & Ni, J. R. 2007 Advanced treatment of coking wastewater by coagulation and zero valent iron process. *Journal of Hazardous Materials* **147**, 232–239.

Lau, I. W., Wang, P. & Fang, H. H. 2001 Organic removal of anaerobically treated leachate by Fenton coagulation. *Journal of Environmental Engineering* **127**(7), 666–669.

Lee, S. & Hur, J. 2016 Heterogeneous adsorption behavior of landfill leachate on granular activated carbon revealed by fluorescence excitation emission matrix (EEM)-parallel factor analysis (PARAFAC). *Chemosphere* **149**, 41–48.

Lei, L., Li, X. & Zhang, X. 2008 Ammonium removal from aqueous solutions using microwave-treated natural Chinese zeolite. *Separation and Purification Technology* **58**(3), 359–366.

Li, X. Z. & Zhao, Q. L. 2001 Efficiency of biological treatment affected by high strength of ammonium-nitrogen in leachate and chemical precipitation of ammonium-nitrogen as pretreatment. *Chemosphere* **44**(1), 37–43.

Li, Y., Wang, S., Shen, Z., Li, X., Zhou, Q., Sun, Y. & Gao, Q. 2020a Gradient adsorption of methylene blue and crystal violet onto compound microporous silica from aqueous medium. *ACS Omega* **5**(43), 28382–28392.

Li, Z., Sun, Y., Yang, Y., Han, Y., Wang, T., Chen, J. & Tsang, D. C. 2020b Biochar-supported nanoscale zero-valent iron as an efficient catalyst for organic degradation in groundwater. *Journal of Hazardous Materials* **383**, 121240.

Liu, C., Bai, R. & San Ly, Q. 2008 Selective removal of copper and lead ions by diethylenetriamine-functionalized adsorbent: behaviors and mechanisms. *Water Research* **42**(6-7), 1511–1522.

Liu, J., Wang, Y., Fang, Y., Mwamulima, T., Song, S. & Peng, C. 2018 Removal of crystal violet and methylene blue from aqueous solutions using the fly ash-based adsorbent material-supported zero-valent iron. *Journal of Molecular Liquids* **250**, 468–476.

Liu, L., Zhao, J., Liu, X., Bai, S., Lin, H. & Wang, D. 2021 Reduction and removal of As (V) in aqueous solution by biochar derived from nano zero-valent-iron (nZVI) and sewage sludge. *Chemosphere* **277**, 130273.

Lopez, A., Pagano, M., Volpe, A. & Di Pinto, A. C. 2004 Fenton's pre-treatment of mature landfill leachate. *Chemosphere* **54**(7), 1005–1010.

Loqman, A., El Bali, B., Lützenkirchen, J., Weidler, P. G. & Kherbeche, A. 2017 Adsorptive removal of crystal violet dye by a local clay and process optimization by response surface methodology. *Applied Water Science* **7**, 3649–3660.

Lou, Z., Dong, B., Chai, X., Song, Y., Zhao, Y. & Zhu, N. 2009 Characterization of refuse landfill leachates of three different stages in landfill stabilization process. *Journal of Environmental Sciences* **21**(9), 1309–1314.

Downloaded from http://iwaponline.com/wpt/article-pdf/doi/10.2166/wpt.2024.029/1374706/wpt2024029.pdf
by guest

Maamoun, I., Eljamal, R., Falyouna, O., Bensaida, K., Sugihara, Y. & Eljamal, O. 2021 Insights into kinetics, isotherms and thermodynamics of phosphorus sorption onto nanoscale zero-valent iron. *Journal of Molecular Liquids* **328**, 115402.

Mahdi, A. E., Ali, N. S., Majdi, H., Albayatia, T. M., Abdulrahman, M. A., Jasim, D. J. & Salih, I. K. 2023 Effective adsorption of 2-nitroaniline from wastewater applying mesoporous material MCM-48: Equilibrium, isotherm, and mechanism investigation. *Desalination and Water Treatment* **300**, 120–129.

Mittal, A. 2006 Adsorption kinetics of removal of a toxic dye, Malachite Green, from wastewater by using hen feathers. *Journal of Hazardous Materials* **133**(1–3), 196–202.

Mortazavian, S., An, H., Chun, D. & Moon, J. 2018 Activated carbon impregnated by zero-valent iron nanoparticles (AC/nZVI) optimized for simultaneous adsorption and reduction of aqueous hexavalent chromium: Material characterizations and kinetic studies. *Chemical Engineering Journal* **353**, 781–795.

Nisticò, R. & Carlos, L. 2019 High yield of nano zero-valent iron (nZVI) from carbothermal synthesis using lignin-derived substances from municipal biowaste. *Journal of Analytical and Applied Pyrolysis* **140**, 239–244.

Nordin, N. I. A. B. A. 2006 *Leachate Treatment Using Constructed Wetland with Magnetic Field*. Master Thesis, Universiti Teknologi Malaysia, Johor. 88 p.

Oloibiri, V., De Coninck, S., Chys, M., Demeestere, K. & Van Hulle, S. W. 2017 Characterisation of landfill leachate by EEM-PARAFAC-SOM during physical-chemical treatment by coagulation-flocculation, activated carbon adsorption and ion exchange. *Chemosphere* **186**, 873–883.

Onundi, Y. B., Mamun, A. A., Al Khatib, M. F. & Ahmed, Y. M. 2010 Adsorption of copper, nickel and lead ions from synthetic semiconductor industrial wastewater by palm shell activated carbon. *International Journal of Environmental Science and Technology* **7**(4), 751–758.

Ozturk, I., Altinbas, M., Koyuncu, I., Arikan, O. & Gomec-Yangin, C. 2003 Advanced physico-chemical treatment experiences on young municipal landfill leachates. *Waste Management* **23**(5), 441–446.

Peng, X., Luan, Z. & Zhang, H. 2006 Montmorillonite–Cu (II)/Fe (III) oxides magnetic material as adsorbent for removal of humic acid and its thermal regeneration. *Chemosphere* **63**, 300–306.

Poguberovic, S. S., Krcmar, D. M., Dalmacija, B. D., Maletic, S. P., Tomasevic-Pilipovic, D. D., Kerkez, D. V. & Roncevic, S. D. 2016 Removal of Ni(II) and Cu(II) from aqueous solutions using 'green' zero-valent iron nanoparticles produced by oak and mulberry leaf extracts. *Water Science and Technology* **74**(9), 2115–2123.

Rathor, G., Chopra, N. & Adhikari, T. 2017 Remediation of nickel ion from soil and water using nano particles of zero-valent iron (nZVI). *Oriental Journal of Chemistry* **33**(2), 1025–1029.

Renou, S., Givaudan, J. G., Poulain, S., Dirassouyan, F. & Moulin, P. 2008 Landfill leachate treatment: Review and opportunity. *Journal of Hazardous Materials* **150**(3), 468–493.

Rodriguez, J., Castrillon, L., Maranon, E., Sastre, H. & Fernandez, E. 2004 Removal of non-biodegradable organic matter from landfill leachates by adsorption. *Water Research* **38**(14-15), 3297–3303.

Ruíz-Baltazar, A., Reyes-López, S. Y., Tellez-Vasquez, O., Esparza, R., Rosas, G. & Pérez, R. 2015 Analysis for the sorption kinetics of Ag nanoparticles on natural clinoptilolite. *Advances in Condensed Matter Physics* **2015**. https://doi.org/10.1155/2015/284518

Sahu, U. K., Tripathy, S., Gouda, N., Mohanty, H. S., Sahu, M. K., Panda, S. P. & Jawad, A. H. 2023 Activated carbon–modified iron oxide nanoparticles for Cr (VI) removal: Optimization, kinetics, isotherms, thermodynamics, regeneration, and mechanism study. *Water, Air, & Soil Pollution* **234**(9), 561.

Stefaniuk, M., Oleszczuk, P. & Ok, Y. S. 2016 Review on nano zerovalent iron (nZVI): From synthesis to environmental applications. *Chemical Engineering Journal* **287**, 618–632.

Sun, P., Hui, C., Azim Khan, R., Du, J., Zhang, Q. & Zhao, Y. H. 2015 Efficient removal of crystal violet using Fe_3O_4-coated biochar: The role of the Fe_3O_4 nanoparticles and modeling study their adsorption behavior. *Scientific Reports* **5**(1), 12638.

Sun, D., Hong, X., Cui, Z., Du, Y., Hui, K. S., Zhu, E. & Hui, K. N. 2020 Treatment of landfill leachate using magnetically attracted zero-valent iron powder electrode in an electric field. *Journal of Hazardous Materials* **388**, 121768.

Tamer, Y. & Berber, H. 2022 Effective removal of crystal violet from aqueous solution by graphene oxide incorporated hydrogel beads as a novel bio-adsorbent: Kinetic, isotherm and thermodynamic studies. *Journal of Macromolecular Science, Part A* **59**(4), 315–328.

Tan, G. Q. & Xiao, D. 2009 Adsorption of cadmium ion from aqueous solution by ground wheat stems. *Journal of Hazardous Materials* **164**, 1359–1363.

Thattil, P. & Leema Rose, A. 2020 Enhanced removal of crystal violet dye using zinc oxide nanorods and air oxidation under sunlight radiation. *Rasayan Journal of Chemistry* **13**(2), 1166–1173.

Ulucan-Altuntas, K., Debik, E., Yoruk, I. I. & Kozal, D. 2017 Single and binary adsorption of copper and nickel metal ions on nano zero valent iron (nZVI): A kinetic approach. *Desalination and Water Treatment* **93**, 274–279.

Wang, G., Li, A. M. & Li, M. Z. 2010a Sorption of nickel ions from aqueous solutions using activated carbon derived from walnut shell waste. *Desalination and Water Treatment* **16**(1–3), 282–289.

Wang, K. S., Lin, C. L., Wei, M. C., Hsui, W. L., Li, H. C., Chang, C. H., Fang, Y. T. & Chang, S. H. 2010b Effect of dissolved oxygen on dye removal by zero valent iron. *Journal of Hazardous Materials* **182**, 886–895.

Wang, C., Luo, H., Zhang, Z., Wu, Y., Zhang, J. & Chen, S. 2014 Removal of As (III) and As (V) from aqueous solutions using nanoscale zero-valent iron-reduced graphite oxide modified composites. *Journal of Hazardous Materials* **268**, 124–131.

Wang, S., Zhao, M., Zhou, M., Li, Y. C., Wang, J., Gao, B. & Ok, Y. S. 2019 Biochar-supported nZVI (nZVI/BC) for contaminant removal from soil and water: A critical review. *Journal of Hazardous Materials* **373**, 820–834.

Downloaded from http://iwaponline.com/wpt/article-pdf/doi/10.2166/wpt.2024.029/1374706/wpt2024029.pdf
by guest

Wang, X., Wang, Y., Shu, Z., Cao, Y., Wang, X., Zhou, F. & Huang, J. 2023 Phenolic hydroxyl-functionalized hyper-cross-linked polymers for efficient adsorptive removal of aniline. *Separation and Purification Technology* **305**, 122443.

Wu, Y. H., Xue, K., Ma, Q. L., Ma, T., Ma, Y. L., Sun, Y. G. & Ji, W. X. 2021 Removal of hazardous crystal violet dye by low-cost P-type zeolite/carbon composite obtained from in situ conversion of coal gasification fine slag. *Microporous and Mesoporous Materials* **312**, 110742.

Yantasee, W., Warner, C. L., Sangvanich, T., Addleman, R. S., Carter, T. G., Wiacek, R. J. & Warner, M. G. 2007 Removal of heavy metals from aqueous systems with thiol functionalized superparamagnetic nanoparticles. *Environmental science & technology* **41**(14), 5114–5119.

Yavuz, O., Altunkaynak, Y. & Guzel, F. 2003 Removal of copper, nickel, cobalt and manganese from aqueous solution by kaolinite. *Water Research* **37**(4), 948–952.

Yi, Z., Huajie, L., Mingchun, L. & Meihua, X. 2020 Adsorption of aniline on aminated chitosan/graphene oxide composite material. *Journal of Molecular Structure* **1209**, 127973.

Yoon, S. Y., Lee, C. G., Park, J. A., Kim, J. H., Kim, S. B., Lee, S. H. & Choi, J. W. 2014 Kinetic, equilibrium and thermodynamic studies for phosphate adsorption to magnetic iron oxide nanoparticles. *Chemical Engineering Journal* **236**, 341–347.

Yuan, P., Liu, D., Fan, M., Yang, D., Zhu, R., Ge, F. & He, H. 2010 Removal of hexavalent chromium [Cr (VI)] from aqueous solutions by the diatomite-supported/unsupported magnetite nanoparticles. *Journal of hazardous materials* **173**(1-3), 614–621.

Yuan, Z., Wang, J., Wang, Y., Liu, Q., Zhong, Y., Wang, Y. & Guo, X. 2019 Preparation of a poly (acrylic acid) based hydrogel with fast adsorption rate and high adsorption capacity for the removal of cationic dyes. *RSC Advances* **9**(37), 21075–21085.

Zhang, J., Gong, J. L., Zenga, G. M., Ou, X. M., Jiang, Y., Chang, Y. N., Guo, M., Zhang, C. & Liu, H. Y. 2016 Simultaneous removal of humic acid/fulvic acid and lead from landfill leachate using magnetic graphene oxide. *Applied Surface Science* **370**, 335–350.

Zhang, C., Jiang, S., Tang, J., Zhang, Y., Cui, Y., Su, C., Qu, Y., Wei, L., Cao, H. & Quan, J. 2018 Adsorptive performance of coal based magnetic activated carbon for perfluorinated compounds from treated landfill leachate effluents. *Process Safety and Environmental Protection* **117**, 383–389. https://doi.org/10.1016/j.psep.2018.05.016.

Zhang, Q., Wang, Y., Wang, Z., Zhang, Z., Wang, X. & Yang, Z. 2021 Active biochar support nano zero-valent iron for efficient removal of U (VI) from sewage water. *Journal of Alloys and Compounds* **852**, 156993.

Zhu, H., Jia, Y., Wu, X. & Wang, H. 2009 Removal of arsenic from water by supported nano zero-valent iron on activated carbon. *Journal of Hazardous Materials* **172**, 1591–1596.

Ziyang, L., Youcai, Z., Tao, Y., Yu, S., Huili, C., Nanwen, Z. & Renhua, H. 2009 Natural attenuation and characterization of contaminants composition in landfill leachate under different disposing ages. *Science of the Total Environment* **407**(10), 3385–3391.

Zou, Y. D., Wang, X. X., Khan, A., Wang, P. Y., Liu, Y. H., Alsaedi, A., Hayat, T. & Wang, X. K. 2016 Environmental remediation and application of nanoscale zero-valent iron and its composites for the removal of heavy metal ions: A review. *Environmental Science and Technology* **50**(14), 7290–7304.

First received 25 August 2023; accepted in revised form 25 January 2024. Available online 12 February 2024

Downloaded from http://iwaponline.com/wpt/article-pdf/doi/10.2166/wpt.2024.029/1374706/wpt2024029.pdf
by guest